

## Electronic Supplementary Information (ESI) for

### **Structural evolution from a fence-like to pillared-layer metal-organic framework for the stable oxygen evolution reaction**

Qian Ren,<sup>a</sup> Jinqi Wu,<sup>a</sup> Jiawei Zhao,<sup>a</sup> Chengfei Li,<sup>a</sup> Li Gong,<sup>b</sup> Dong-Dong Zhou,<sup>\*a</sup> and Gao-Ren Li<sup>\*a</sup>

<sup>a</sup>MOE Key Laboratory of Bioinorganic and Synthetic Chemistry, School of Chemistry, Sun Yat-Sen University, Guangzhou 510275, China

<sup>b</sup>Instrumental Analysis and Research Center, Sun Yat-Sen University, Guangzhou 510275, China

\*E-mails: zhoudd3@mail.sysu.edu.cn; ligaoren@mail.sysu.edu.cn

#### **Materials and Methods**

##### **Materials**

All the chemicals used were analytical grade (AR) and utilized without any additional purification.

##### **Synthesis of [Co<sub>3</sub>(OH)<sub>2</sub>(fum)<sub>2</sub>(H<sub>2</sub>O)<sub>4</sub>]·2H<sub>2</sub>O (Co<sub>3</sub>-fum<sub>2</sub>)**

Fumaric acid (H<sub>2</sub>fum, 174 mg, 1.5 mmol) and KOH (206 mg, 3.5 mmol) were dissolved in deionized water (2.5 mL) to obtain a homogeneous solution, then CoCl<sub>2</sub> (237 mg, 1 mmol) was added under continuous stirring at 25 °C for 1 h until forming uniform suspension. The pink powder of Co<sub>3</sub>-fum<sub>2</sub> was gained and washed with ethanol and distilled water for several times, and dried at 60 °C.

##### **Synthesis of [Co<sub>4</sub>(OH)<sub>6</sub>(fum)<sub>2</sub>] (Co<sub>4</sub>-fum<sub>2</sub>)**

H<sub>2</sub>fum (70 mg, 0.6 mmol) and NaOH (50 mg, 1.2 mmol) were dissolved in deionized water (20 mL), and then treated with ultrasonic bath for 30 min to obtain a homogeneous solution. Co(NO<sub>3</sub>)<sub>2</sub> (175 mg, 0.6 mmol) was added under continuous stirring until dissolved. The above mixture solvent was transferred a Teflon-lined stainless-steel autoclave, then the autoclave was sealed and maintained at 180 °C for 12 h. The tawny color powder of Co<sub>4</sub>-fum<sub>2</sub> were gained and centrifugation washed with ethanol and distilled water for several times, and dried at 60 °C. (yield: 17.0%, based on Co salt). Other method (post-synthesis): Co<sub>3</sub>-fum<sub>2</sub> (50 mg) was dispersed to 5 mL CoCl<sub>2</sub> aqueous solution (5 mM) to form a uniform suspension, the above suspension was transferred into a Teflon-lined

stainless-steel autoclave (20 mL) at 180 °C for 12 h. Finally, the resultant precipitate with tawny color was collected by centrifugation and rinsed with ethanol and distilled water for several times, and dried at 60 °C (yield: 69.8%, based on  $\text{Co}_3\text{-fum}_2$ ).

#### **Synthesis of $\text{Co}_4\text{-fum}_2/\text{NF}$ arrays**

The preparation method is the same as the as-synthesized procedure, except for lower feed:  $\text{H}_2\text{fum}$  (116 mg, 1 mmol) and NaOH (80 mg, 2 mmol) were dissolved in 25 mL deionized water, and then treated with ultrasonic bath for 30 min to obtain a homogeneous solution. 1 mmol  $\text{Co}(\text{NO}_3)_2$  was added under continuous stirring until dissolved. The above mixture solvent was transferred a Teflon-lined stainless-steel autoclave (50 mL), where a piece of as-prepared NF ( $3 \times 3 \text{ cm}^2$ ) was immersed into the solution at 180 °C for 24 h. And the electrode of  $\text{Co}_4\text{-fum}_2/\text{NF}$  was obtained by washing with ethanol and distilled water for several times, and dried at 60 °C, loading mass:  $4.9 \text{ mg cm}^{-2}$ .

#### **Synthesis of $\text{Co}_{3.5}\text{Fe}_{0.5}\text{-fum}_2/\text{NF}$ arrays**

A piece of  $\text{Co}_4\text{-fum}_2/\text{NF}$  ( $1 \times 2 \text{ cm}^2$ ) was immersed in 10 mL 0.02 M  $\text{Fe}(\text{NO}_3)_3$  solution and maintained for 2 h at 25 °C. The electrode of  $\text{Co}_{3.5}\text{Fe}_{0.5}\text{-fum}_2/\text{NF}$  was obtained by washing with ethanol and distilled water for several times to remove residual  $\text{Fe}(\text{NO}_3)_3$  solution on surfaces, and dried at 60 °C. ICP-AES results also showed that the molar ratio of Co:Fe is about 3.5:0.5 (hereafter denoted as  $\text{Co}_{3.5}\text{Fe}_{0.5}\text{-fum}_2/\text{NF}$ ), loading mass:  $3.7 \text{ mg cm}^{-2}$ .

#### **Synthesis of $\text{Co}(\text{OH})_2$**

In a typical hydrothermal method,  $\text{CoCl}_2 \cdot 6\text{H}_2\text{O}$  (237 mg, 1 mmol) was dissolved in deionized water (15 mL),  $\text{N}_2\text{H}_4 \cdot \text{H}_2\text{O}$  (80 wt%, 1 mL) was added to the solution as alkaline conditioner. The solution was transferred to a sealed Teflon-lined autoclave and then heated at 120 °C for 12 h. After cool to room temperature, the product was collected by centrifugation and washed several times with deionized water and ethanol, and dried at 60 °C.

#### **Methods**

The Ni foam (NF) ( $3 \times 3 \text{ cm}^2$ ) was rinsed with ethanol in ultrasonic bath for 30 min, and then immersed in the 3 M hydrochloric acid (HCl) solution for 2 h, the obtained NF was washed repeatedly with distilled water. Powder X-ray diffraction (PXRD) patterns were obtained on a Rigaku D/Max 2550 X-ray diffractometer at 40 kV and 30 mA. The surface morphologies and inner structure of the products were characterized by Zeiss Sigma field emission scanning electron microscope (FE-

SEM, Quanta 400FEG) and transmission electron microscope (TEM, JEM-2010HR) and high-resolution TEM (HRTEM, JEM-3010HR). Atomic force microscopy (AFM) images were obtained by a SHIMADZU SPM-9500J3 device. The chemical-state analysis of catalysts was performed by X-Ray photoelectron spectroscopy (XPS) using an ESCAKAB 250 X-Ray photoelectron spectrometer. All the XPS spectra peaks were corrected by C 1s line at 284.8 eV as standard, and curve fitting and background subtraction were accomplished. Molecular groups analysis of samples was determined by Fourier transform infrared (FTIR) spectra (Renishaw inVia). Thermogravimetric analysis (TG) was measured using a TG209F1 libra system under N<sub>2</sub>, over a range of 25–800 °C with heating rate of 10 °C min<sup>-1</sup>. The elemental analyses (C, H, N) was recorded with a Vario EL elemental analyzer. The inductively coupled plasma-atomic emission spectrometry (ICP-AES) was carried out on TJA IRIS (HR) spectrometer.

Simulation of crystal morphology was performed by Bravais, Friedel, Donnay and Harker (BFDH) method using Mercury software (CSD software package). To display BFDH theoretical crystal morphologies, hit *CSD-Materials* and then *Calculations* in the top-level menu, then *BFDH Morphology*.

### **Electrochemical measurements**

All electrocatalysts measurements were performed in a three-compartment electrochemical glass cell at room temperature using a CHI 660D Electrochemical Workstation in the O<sub>2</sub>-saturated solution. A glassy carbon (GC) electrode (3 mm in diameter) or Ni foam (the area in the submerged electrolyte is 0.2 × 0.5 cm<sup>2</sup>) was used as the working electrode, all potentials were referenced to a Hg/HgO (1 M KOH) electrode as reference electrode, and carbon rod as the counter electrode in all measurements. The powder catalyst suspension was prepared using mixture of 0.5 mL 0.25 wt% nafion ethanol solution and 8 mg catalysts and 1 mg carbon black powder followed by ultrasonication for 30 min. Then, 4 μL of the above ink was uniformly dropped on a freshly polished GC electrode, and then dried at room temperature. When the Co<sub>4</sub>-fum<sub>2</sub>/NF and Co<sub>3.5</sub>Fe<sub>0.5</sub>-fum<sub>2</sub>/NF networks arrays were used as the working electrode, the area of the submerged part was 0.2 cm<sup>2</sup> (0.2 cm × 0.5 cm × 2). All potentials measured were referenced to the reversible hydrogen electrode (RHE) using the following equation:  $E_{\text{RHE}} \text{ (V)} = E_{\text{Hg/HgO}} \text{ (V)} + 0.098 \text{ V} + 0.059 \text{ pH}$ . The OER overpotential ( $\eta$ ) was calculated according to the formula:  $\eta = E_{\text{RHE}} - 1.22 \text{ V}$ . The linear sweep voltammetry (LSV) was performed at

a scan rate of  $5 \text{ mV s}^{-1}$  (for powder catalysts) and  $1 \text{ mV s}^{-1}$  (for  $\text{Co}_4\text{-fum}_2/\text{NF}$  and  $\text{Co}_{3.5}\text{Fe}_{0.5}\text{-fum}_2/\text{NF}$  arrays) in  $1.0 \text{ M KOH}$  (pH 14) solution (the deionized water was used as solvent). All polarization curves were corrected with 95% iR-compensation.

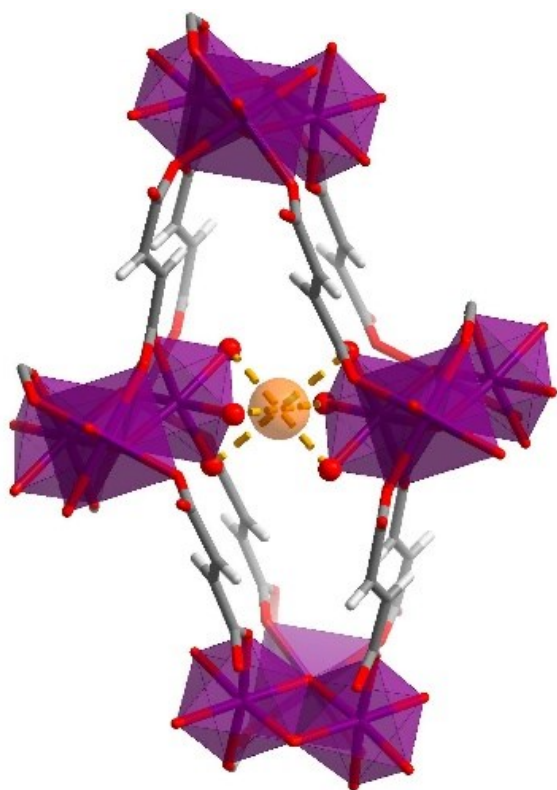


**Fig. S1** The local environment of coordinated water orienting into the 1D pore channel in  $\text{Co}_3\text{-fum}_2$  (transparent yellow ball is the center of six coordinated water molecules).

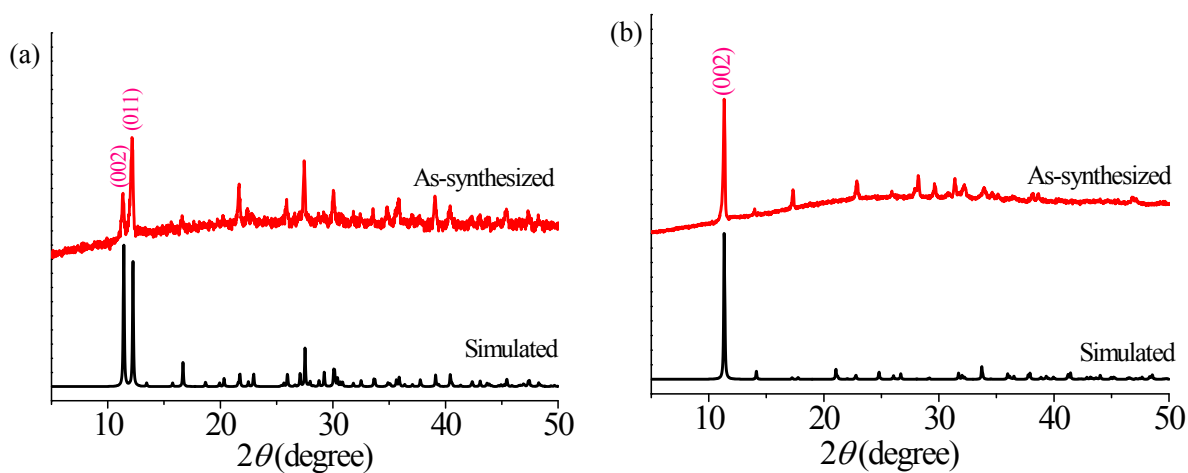


**Fig. S2** PXRD patterns of (a)  $\text{Co}_3\text{-fum}_2$  and (b)  $\text{Co}_4\text{-fum}_2$ .



**Fig. S3** Product color of (a)  $\text{Co}_3\text{-fum}_2$  and (b)  $\text{Co}_4\text{-fum}_2$  powder.

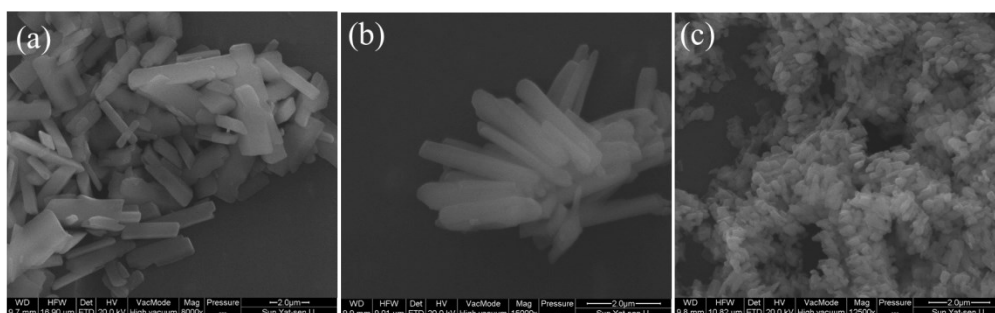


**Fig. S4** SEM images of (a)  $\text{Co}_3\text{-fum}_2$ , (b)  $\text{Co}_4\text{-fum}_2$  and (c)  $\text{Co}_4\text{-fum}_2$  of post-synthesis.

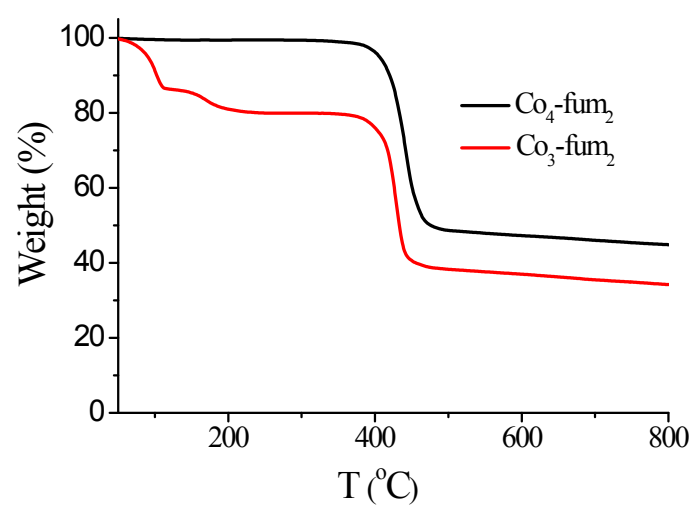


**Fig. S5** TG curves of  $\text{Co}_3\text{-fum}_2$  and  $\text{Co}_4\text{-fum}_2$  powder.

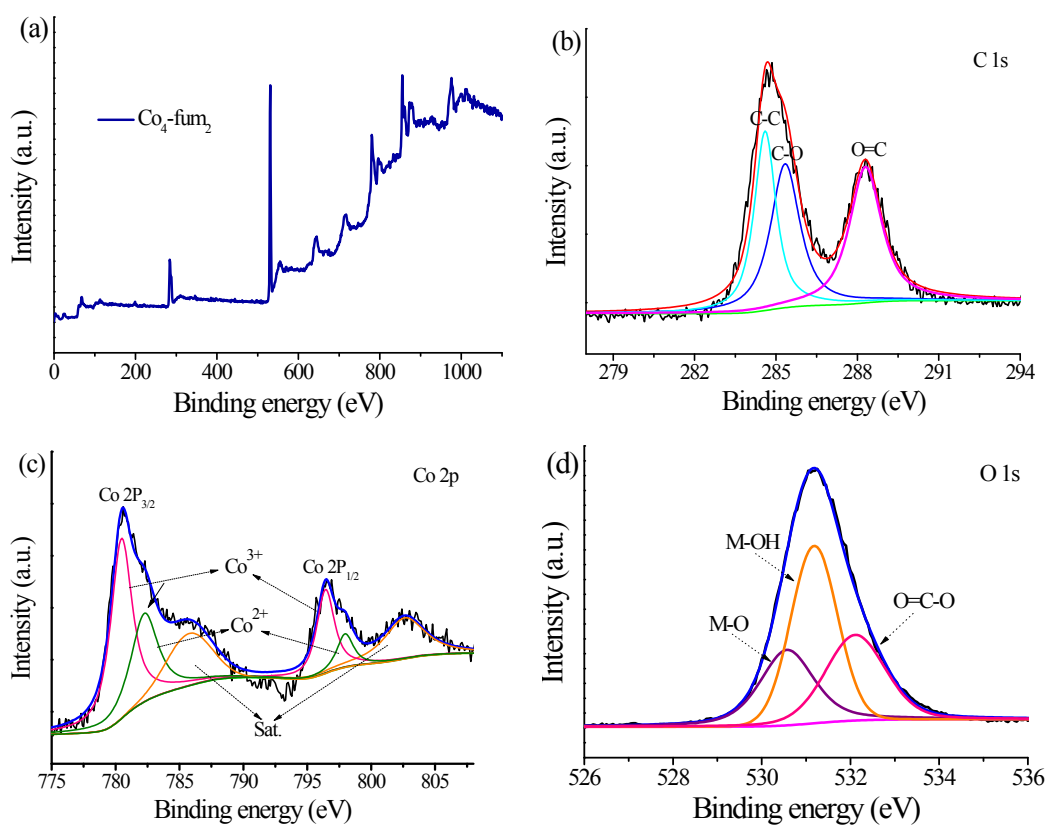


**Fig. S6** (a) XPS survey spectra, High-resolution XPS spectra of (b) C 1s, (c) Co 2p and (d) O1s in  $\text{Co}_4\text{-fum}_2$ .

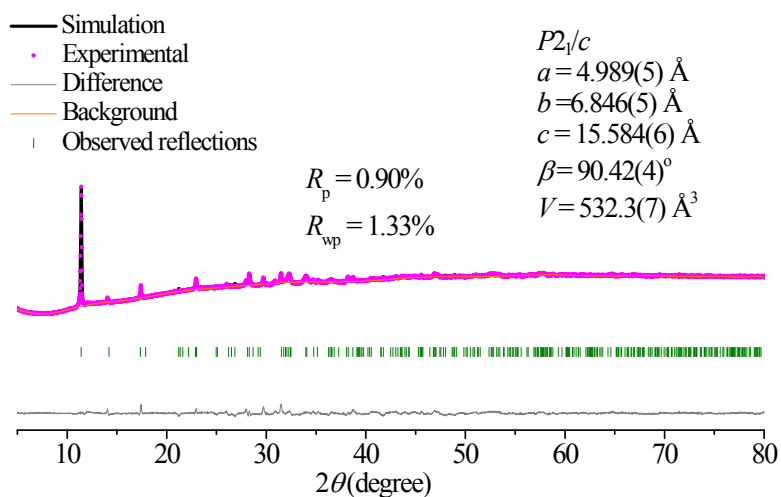


**Fig. S7** Final Rietveld refinement results of  $\text{Co}_4\text{-fum}_2$ .

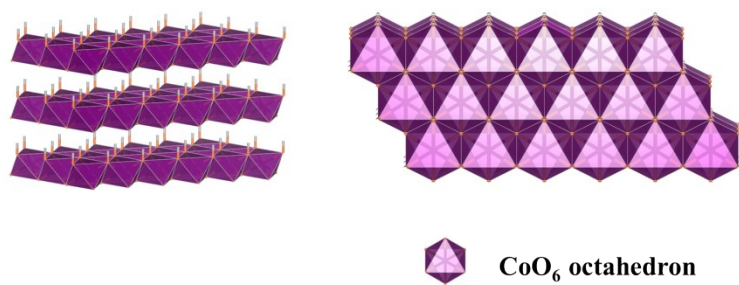


**Fig. S8** Schematic diagram of cobalt hydroxide structure.

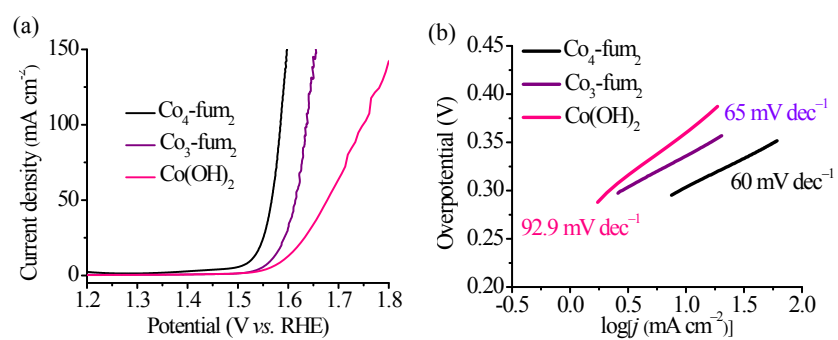


**Fig. S9** (a) LSV curves and (b) Tafel curves of Co<sub>3</sub>-fum<sub>2</sub> and Co<sub>4</sub>-fum<sub>2</sub> on GCE.

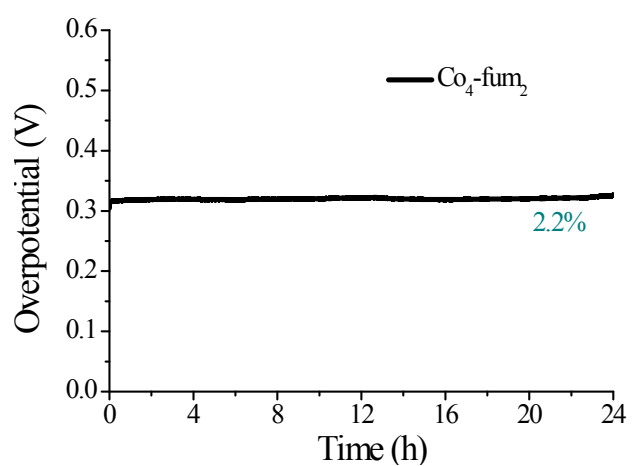


**Fig. S10** E-t curves of Co<sub>4</sub>-fum<sub>2</sub> powder.

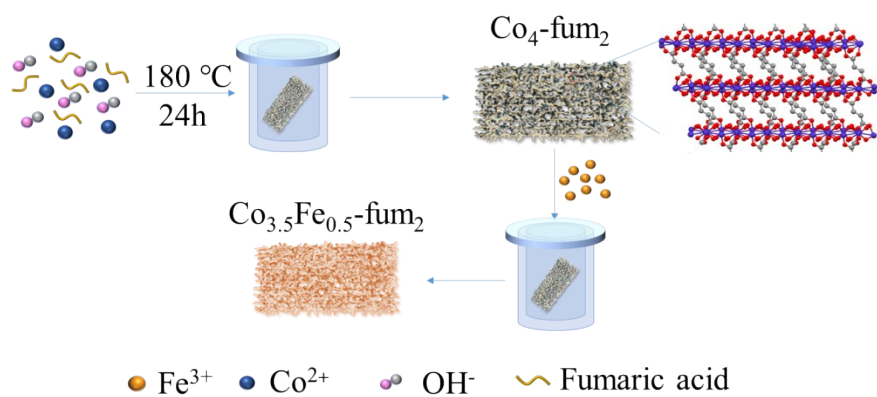


**Fig. S11** Illustration of the fabrication of  $\text{Co}_4\text{-fum}_2/\text{NF}$  and  $\text{Co}_{3.5}\text{Fe}_{0.5}\text{-fum}_2/\text{NF}$ .

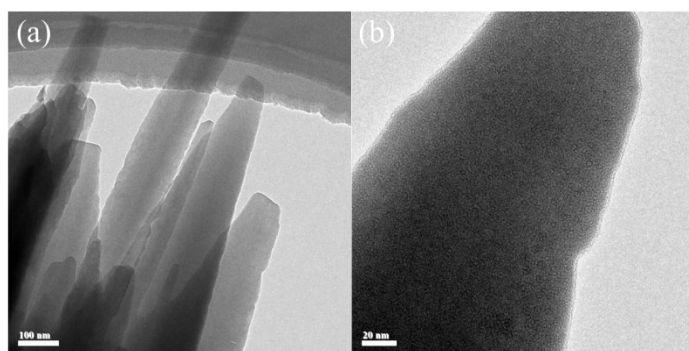


**Fig. S12** TEM images of  $\text{Co}_4\text{-fum}_2/\text{NF}$ .

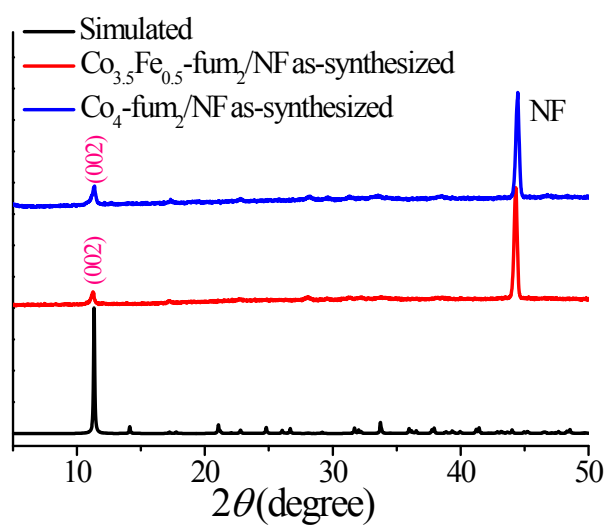


**Fig. S13** PXRD patterns of  $\text{Co}_4\text{-fum}_2/\text{NF}$  and  $\text{Co}_{3.5}\text{Fe}_{0.5}\text{-fum}_2/\text{NF}$ .

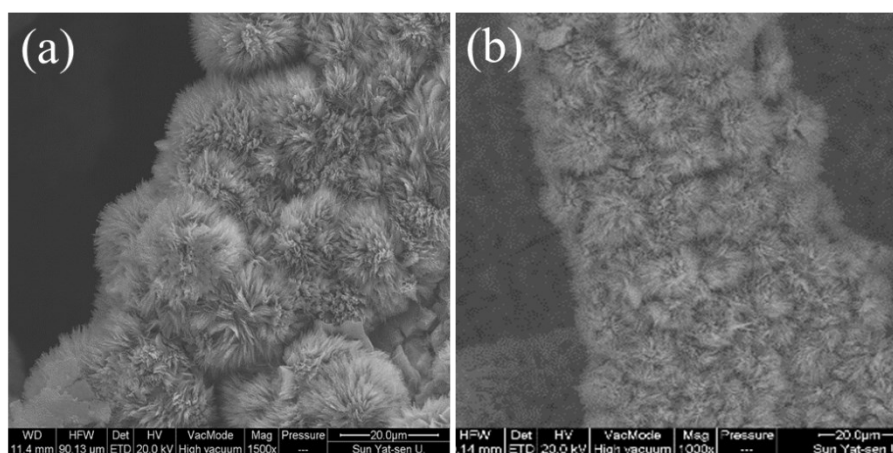


**Fig. S14** SEM images of (a)  $\text{Co}_4\text{-fum}_2/\text{NF}$  and (b)  $\text{Co}_{3.5}\text{Fe}_{0.5}\text{-fum}_2/\text{NF}$  after OER test in 1.0 M KOH solution.

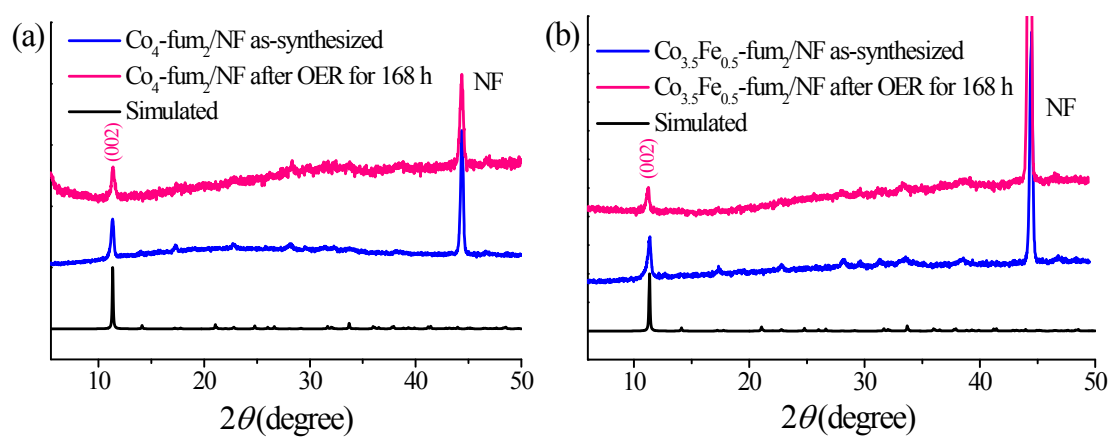


**Fig. S15** XRD patterns of (a)  $\text{Co}_4\text{-fum}_2/\text{NF}$  and (b)  $\text{Co}_{3.5}\text{Fe}_{0.5}\text{-fum}_2/\text{NF}$  after OER test in 1.0 M KOH solution.

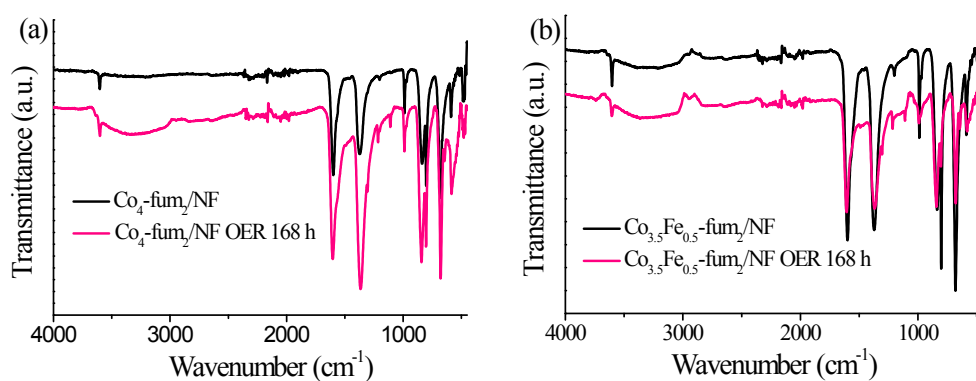


**Fig. S16** FTIR spectra of (a)  $\text{Co}_4\text{-fum}_2/\text{NF}$  and (b)  $\text{Co}_{3.5}\text{Fe}_{0.5}\text{-fum}_2/\text{NF}$  after 168h OER test in 1.0 M KOH solution.

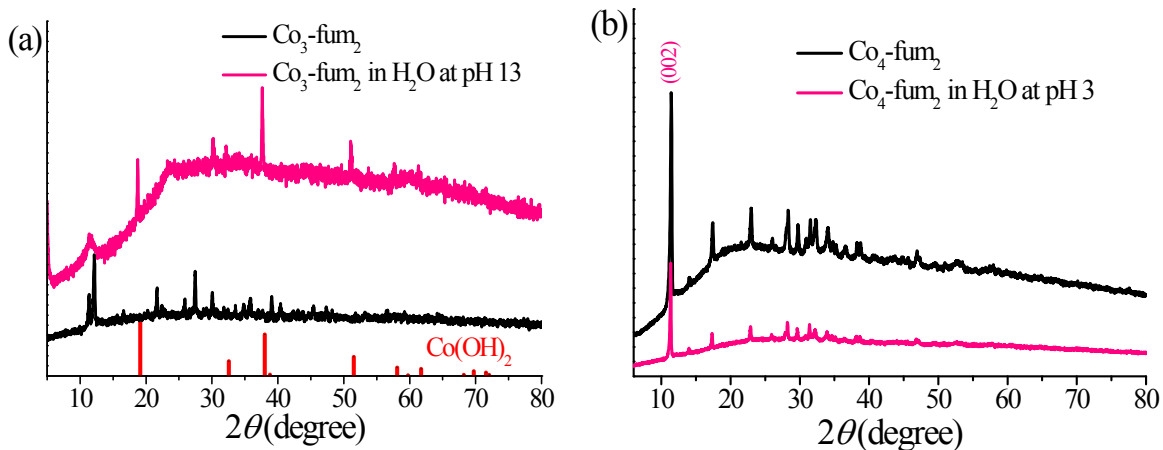


**Fig. S17** PXRD patterns of (a)  $\text{Co}_3\text{-fum}_2$  immersed in 0.1M KOH solutions (pH 13) for 12 h and (b)  $\text{Co}_4\text{-fum}_2$  immersed in  $\text{H}_2\text{SO}_4$  solutions (pH 3) for 24 h at room temperature.

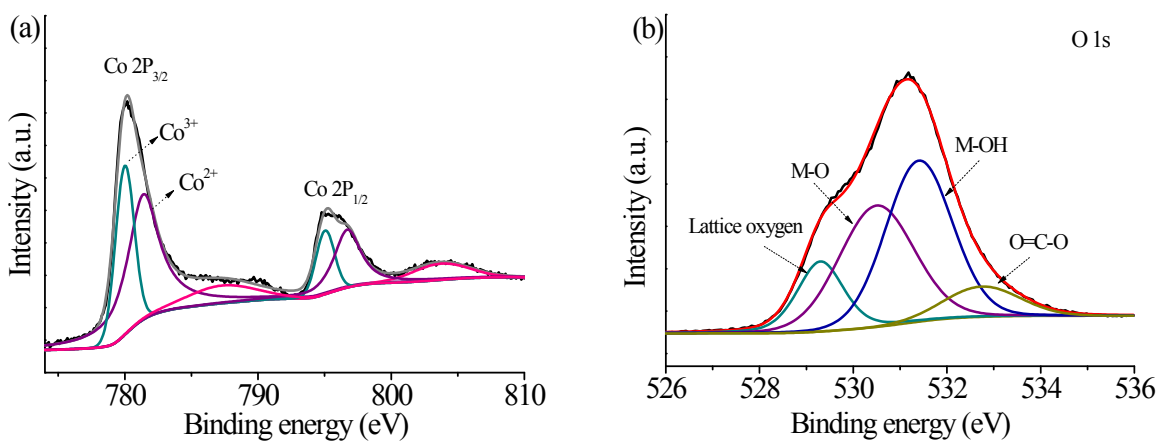


**Fig. S18** High-resolution (a) Co 2p and (b) O 1s XPS spectra of  $\text{Co}_4\text{-fum}_2$  that collected from the surface of the  $\text{Co}_4\text{-fum}_2/\text{NF}$  after OER by ultrasound.

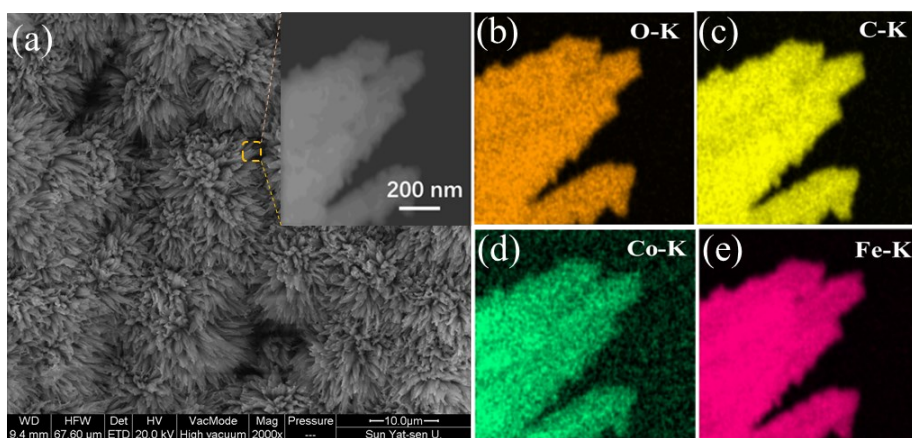


**Fig. S19** (a) SEM images and (b-e) element mappings of  $\text{Co}_{3.5}\text{Fe}_{0.5}\text{-fum}_2/\text{NF}$  (the corresponding region is shown in the insert of (a)).

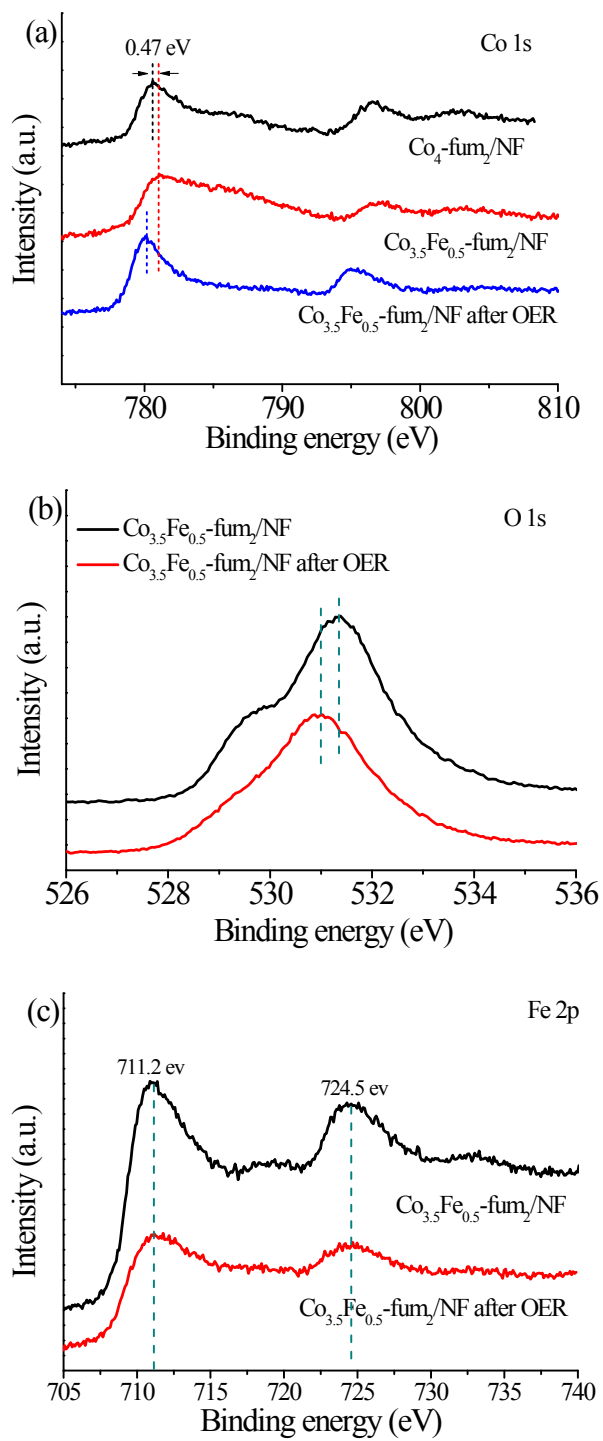


**Fig. S20** High-resolution (a) Co 2p, (b) O 1s and (c) Fe 2p XPS spectra of Co<sub>3.5</sub>Fe<sub>0.5</sub>-fum<sub>2</sub>/NF before and after OER test.

**Table S1.** The summary of MOFs electrocatalysts for OER.

MOFs types	Substrate	Electrolyte	$\eta_{10}$ /mA cm <sup>-2</sup> /mV	Tafel slope / mV deg <sup>-1</sup>	Refs
NiCo-UMOFNs	GCE	1.0 M KOH	250 <sub>/10</sub>	42	[1]
Co-UMOFNs			371 <sub>/10</sub>	103	
Co <sub>2</sub> (OH) <sub>2</sub> BDC	GCE	1.0 M KOH	263 <sub>/10</sub>	74	[2]
Co <sub>3</sub> O <sub>4</sub> @Co-MOF-12	GCE	1.0 M KOH	277 <sub>/10</sub>	79	[3]
Co-MOF			359 <sub>/10</sub>	95	
A <sub>2.7</sub> B-MOF-FeCo <sub>1.6</sub>	GCE	1.0 M KOH	288 <sub>/10</sub>	39	[4]
MAF-X27-OH	GCE	1.0 M KOH	292 <sub>/10</sub>	---	[5]
Co-MOF ([Co <sub>4</sub> (OH) <sub>2</sub> ] <sup>6+</sup> )	GCE	1.0 M KOH	318 <sub>/10</sub>	54	[6]
Co-ZIF-9 (nanosheets)	GCE	1.0 M KOH	380 <sub>/10</sub>	55	[7]
[Ni <sub>3</sub> (OH) <sub>2</sub> (BDC) <sub>2</sub> (H <sub>2</sub> O) <sub>4</sub> ·2H <sub>2</sub> O	GCE	1.0 M KOH	386 <sub>/10</sub>	106.1	[8]
NiFe-MOF	GCE	0.1 M KOH	406 <sub>/10</sub>	56	[9]
MIL-53(FeNi)	NF	1.0 M KOH	233 <sub>/50</sub>	31.4	[10]
MIL-53(Ni)			309 <sub>/50</sub>	39.6	
(Ni <sub>2</sub> Co <sub>1</sub> ) <sub>0.925</sub> Fe <sub>0.075</sub> -MOF	NF	1.0 M KOH	257 <sub>/10</sub>	41.3	[11]
Ni-MOF-74	NF	1.0 M KOH	313 <sub>/10</sub>	134.1	[12]
NiFe-MOF-74			223 <sub>/10</sub>	71.6	
Co-MOF	NF	1.0 M KOH	311 <sub>/50</sub>	77	[13]
Fe:2D-Co-NS	NF	0.1 M KOH	211 <sub>/10</sub>	46	[14]
2D-Co-NS	NF		255 <sub>/10</sub>	65	
Fe <sub>3</sub> -Co <sub>2</sub>	NF	0.1 M KOH	225 <sub>/10</sub>	48	[15]
2D NiFe-MOF	NF	0.1 M KOH	240 <sub>/10</sub>	34	[9]
Ni-MOF			296 <sub>/10</sub>	45	
Fe/Ni-BTC film	NF	0.1 M KOH	270 <sub>/10</sub>	47	[16]
Co <sub>4</sub> -fum <sub>2</sub>	GCE	1.0 M KOH	309 <sub>/10</sub>	60.1	This work
Co <sub>4</sub> -fum <sub>2</sub>	NF	1.0 M KOH	267 <sub>/10</sub>	63	This work
Co <sub>3.5</sub> Fe <sub>0.5</sub> -fum <sub>2</sub>	NF	1.0 M KOH	238 <sub>/10</sub>	44	This work

A = terephthalic ligand; B = 2-aminoterephthalic acid; GCE: Glassy carbon electrode; CB: Carbon cloth; NF: Nickel foam; CF: Copper foam.

## References

- [1] S. L. Zhao, Y. Wang, J. C. Dong, C. T. He, H. J. Yin, P. F. An, K. Zhao, X. F. Zhang, C. Gao, L. J. Zhang, J. W. Lv, J. X. Wang, J. Q. Zhang, A. M. Khattak, N. A. Khan, Z. X. Wei, J. Zhang, S. Q. Liu, H. J. Zhao, Z. Y. Tang, *Nat. Energy*, 2016, **1**, 16184.
- [2] Y. X. Xu, B. Li, S. S. Zheng, P. Wu, J. Y. Zhan, H. G. Xue, Q. Xu, H. Pang, *J. Mater. Chem. A*, 2018, **6**, 22070.
- [3] S. S. Zheng, X. T. Guo, H. G. Xue, K. M. Pan, C. S. Liu, H. Pang, *Chem. Commun.*, 2019, **55**, 10904.
- [4] Z. Q. Xue, Y. L. Li, Y. W. Zhang, W. Geng, B. M. Jia, J. Tang, S. X. Bao, H. P. Wang, Y. N. Fan, Z. W. Wei, Z. S. Zhang, Z. F. Ke, G. Q. Li, and C. Y. Su, *Adv. Energy Mater.*, 2018, **8**, 1801564.
- [5] X. F. Lu, P. Q. Liao, J. W. Wang, J. X. Wu, X. W. Chen, C. T. He, J. P. Zhang, G. R. Li, X. M. Chen, *J. Am. Chem. Soc.*, 2016, **138**, 8336.
- [6] X. L. Song, C. D. Peng, H. H. Fei, *ACS Appl. Energy Mater.*, 2018, **1**, 2446.
- [7] K. Jayaramulu, J. Masa, D. M. Morales, O. Tomanec, V. Ranc, M. Petr, P. Wilde, Y. T. Chen, R. Zboril, W. Schuhmann, R. A. Fischer, *Adv. Sci.*, 2018, **5**, 1801029.
- [8] F. L. Li, P. T. Wang, X. Q. Huang, D. J. Young, H. F. Wang, P. Braunstein, J. P. Lang, *Angew. Chem. Int. Ed.*, 2019, **131**, 7125.
- [9] J. J. Duan, S. Chen, C. Zhao, *Nat. Commun.*, 2017, **8**, 15341.
- [10] F. Z. Sun, G. Wang, Y. Q. Ding, C. Wang, B. B. Yuan, Y. Q. Lin, *Adv. Energy Mater.*, 2018, **8**, 1800584.
- [11] Q. Z. Qian, Y. P. Li, Y. Liu, L. Yu, G. Q. Zhang, *Adv. Mater.*, 2019, **31**, 1901139.
- [12] J. L. Xing, K. L. Guo, Z. H. Zou, M. M. Cai, J. Du, C. L. Xu, *Chem. Commun.*, 2018, **54**, 7046.
- [13] X. Q. Zhang, W. D. Sun, H. T. Du, R. M. Kong, F. L. Qu, *Inorg. Chem. Front.*, 2018, **5**, 344.
- [14] J. Huang, Y. Li, R. K. Huang, C. T. He, L. Gong, Q. Hu, L. S. Wang, Y. T. Xu, X. Y. Tian, S. Y. Liu, Z. M. Ye, F. X. Wang, D. D. Zhou, W. X. Zhang, J. P. Zhang, *Angew. Chem. Int. Ed.*, 2018, **130**, 4722.
- [15] J. Q. Shen, P. Q. Liao, D. D. Zhou, C. T. He, J. X. Wu, W. X. Zhang, J. P. Zhang, X. M. Chen, *J. Am. Chem. Soc.*, 2017, **139**, 1778.
- [16] L. Wang, Y. Z. Wu, R. Cao, L. T. Ren, M. X. Chen, X. Feng, J. W. Zhou, B. Wang, *ACS Appl. Mater. Interfaces*, 2016, **8**, 16736.